The Lunar Breccia Dhofar 1442: Noble Gases, Nitrogen, and Carbon Released by Stepwise Combustion and Crushing

ISSN 0016-7029, Geochemistry International, 2022, Vol. 60, No. 12, pp. 1192–1206. © The Author(s), 2022. This article is an open access publication.
Russian Text © The Author(s), 2022, published in Geokhimiya, 2022, Vol. 67, No. 12, pp. 1184–1200.

The Lunar Breccia Dhofar 1442: Noble Gases, Nitrogen, and Carbon Released by Stepwise Combustion and Crushing

E. V. Korochantseva[a], *, A. B. Verchovsky[b], and A. V. Korochantsev[a]

[a] *Vernadsky Institute of Geochemistry and Analytical Chemistry, Russian Academy of Sciences, Moscow, 119991 Russia*
[b] *School of Physical Sciences, The Open University, Milton Keynes, MK7 6AA, UK*
**e-mail: kpv-life@mail.ru*

Received June 30, 2022; revised July 14, 2022; accepted July 15, 2022

Abstract—Stepwise crushing and combustion methods were applied to study the KREEP-rich lunar breccia Dhofar 1442, the clastic material of which is cemented by porous matrix. The stepwise crushing released significant amount of gases of extraterrestrial origin from gas voids. Argon, nitrogen, and carbon are simultaneously released by stepwise combustion at 1100°C. The simultaneous high-temperature degassing of these gases, as well as the coincidence of C/N ratio and nitrogen and carbon contents in high-temperature combustion steps with those of crushing indicate that the gas carriers are voids in high-temperature phases (in particular, minerals, glasses), which are decomposed/melted at these temperatures. Helium and neon are released from the same positions at lower temperatures. The isotopic composition of neon obtained by stepwise combustion and crushing corresponds to the composition of fractionated solar wind. The fraction of argon in the first crushing steps is higher than that of any other of studied gases. The $^{40}Ar/^{36}Ar$ in the trapped lunar argon is ~18, which is not consistent with empirical model implying that ^{40}Ar is implanted from lunar atmosphere (McKay et al., 1986; Eugster et al., 2001; Joy et al., 2011). We believe that the entrapment of volatile elements in gas voids of the meteorite Dhofar 1442 was caused by the redistribution of gases from one structural sites into others during impact events that accompanied the cratering, in particular, leading to the formation of the impact melt breccia Dhofar 1442. The trapped gases of the meteorite Dhofar 1442 contain not only typical volatile components (solar, radiogenic, cosmogenic, re-implanted ^{40}Ar) of lunar breccias, but also nitrogen and carbon formed through the oxidation of organic matter of metamorphosed chondrites, which are present in the breccia. With increasing number of strokes and, correspondingly, a degree of crushing, the elemental ratios change. A slight decrease of $^{4}He/^{20}Ne$ ratio during crushing is likely related to the different diffusion ability and permeability of helium relative to neon under temperature influence and/or to the heterogeneous distribution of these gases in voids of different size. The $^{4}He/^{36}Ar$, $^{20}Ne/^{36}Ar$, $^{14}N/^{36}Ar$, and $^{12}C/^{36}Ar$ ratios increase by factors of 10–100 during crushing. This can be explained by the combination of dynamically different processes leading to the argon fractionation relative to other gases and uneven redistribution of gases from different positions in voids of different sizes during impact metamorphism.

Keywords: meteorites, lunar breccia, regolith, noble gases, nitrogen, carbon, stepwise crushing and combustion

DOI: 10.1134/S0016702922120035

INTRODUCTION

Meteorites that came on Earth from the Moon provide insight into natural processes in the Moon's interior and the rock transformations in the surface layer of their parent body. Isotopic compositions of volatile elements serve as important tracers in deciphering the conditions of formation of extraterrestrial matter and the environment in which it evolved. We have recently studied the isotopic composition and elemental ratios of noble gases, nitrogen, and carbon in the lunar meteorite Dhofar 1436 using stepwise pyrolysis, combustion and stepwise crushing applied to a lunar meteorite for the first time (Korochantseva et al., 2021). Unlike terrestrial rocks, the extraterrestrial material is rarely analyzed by stepwise crushing technique, because many types of meteorites are depleted in volatiles that could be extracted from gas voids (gas inclusions and vesicles, cosmogenic and radiogenic tracks, and other defects in mineral structure, hereinafter referred to as voids) by crushing. However, lunar breccias could accumulate very high gas concentrations in microvoids during regolith processes, as is the case with the meteorite Dhofar 1436 (Korochantseva et al., 2021), in which isotopic-geochemical features of gas phase trapped on the Moon during post-impact processes were determined. The latter processes involve a change of pressure and temperature, fracturing, degassing, melting and evaporation, gas diffusion, formation of high-pressure phases, thermal metamorphism caused by heating of the material, and others.

Korochantseva et al., 2021 demonstrated that a combination of applied methods is a promising tool for studying highly volatile elements in the lunar material. According to the preliminary results of ^{40}Ar–^{39}Ar dating of some lunar meteorites (Korochantseva et al., 2016a), the KREEP-rich regolith breccia Dhofar 1442 with porous matrix (Weisberg et al., 2009; Korotev et al., 2009; Demidova et al., 2014) has the elevated concentrations of argon, and hence, represents a promising object for further geochemical and isotopic study of highly volatile elements and their compounds behavior during transformation of lunar soil. For this purpose, we carried out isotope studies of noble gases (He, Ne, Ar), nitrogen and carbon released by stepwise combustion and crushing methods from the lunar meteorite Dhofar 1442 samples and report the obtained results in this work.

METEORITE DESCRIPTION

The lunar meteorite Dhofar 1442 was found in the desert of the Dhofar province (Oman) in 2005 (Weisberg et al., 2009). Five stones were found within two meters from each other. The samples lack fusion crust and were only insignificantly weathered (Weisberg et al., 2009).

The meteorite was classified as an impact melt breccia (Weisberg et al., 2009) with some features resembling regolith breccia (Demidova et al., 2012). However, in some studies (Korotev et al., 2009; Zeigler et al., 2011) Dhofar 1442 is classified as the regolith breccia based on the presence of glassy spherules (Stöffler et al., 1980). In any case, this is one of the KREE-richest lunar meteorites. The KREEP component is characterized by the high contents of incompatible elements, which is associated with the presence of phosphates, zircon, and K-feldspar. Dhofar 1442 contains both highland and mare material (Demidova et al., 2012; Yang et al., 2019). Such lunar breccias containing a mixture of anorthosites, basalts, and/or KREEP material are ascribed to a group of "mixed" lunar meteorites (Korotev et al., 2022a). According to the classification (Korotev et al., 2022b), the meteorite Dhofar 1442 falls in the group of "Th-rich (>3.5 ppm), moderately mafic breccias".

Dhofar 1442 contains numerous clasts of rocks (0.02–8 mm), minerals, and glasses embedded in a brownish glassy porous impact melt matrix (Weisberg et al., 2009; Demidova et al., 2014). The matrix/clast ratio varies from sample to sample; in some domains (up to 0.5 mm), the clasts are practically absent (Weisberg et al., 2009; Demidova et al., 2014). The lithic clasts include basalts, granophyres, impact melt breccias, granulites, gabbros, olivine gabbro-norites, gabbro-norites, norites, agglutinates, and anorthosites (Weisberg et al., 2009; Zeigler et al., 2011). The anorthosite clasts are common of highland breccias but are practically absent in this meteorite (Korotev et al., 2009). The most abundant lithic clasts are the KREEP-bearing norites and gabbro-norites (Demidova et al., 2014). These authors noted that the meteorite Dhofar 1442 also contains low-Ti basalts, felsic rocks, and fragments of impact melt breccias. In the latter, the lithic and mineral clasts (<30%) are chemically almost identical to those of the groundmass, and are cemented by impact melt matrix, which differs from the meteorite matrix in color and texture. The mineral fragments are mainly represented by pyroxene and plagioclase, which show wider compositional variations than those in the studied lithic clasts. The less abundant mineral fragments are ilmenite, olivine, silica phases, K-feldspar, apatite, merrilite, spinel-group minerals, and spinel-ilmenite intergrowths with fine lamellar or wedge-shaped rutile. Troilite, Fe–Ni metal, and unusual intergrowth of ilmenite, Cr–Zr–Ca–B armalcolite, baddeleyite, rutile, and Al–Ti-chromite occur in accessory amounts. Glass or cryptocrystalline material is present in meteorite matrix or as separate clasts (Demidova et al., 2014). Glasses in the meteorite have felsic (clasts 10–500 μm in size), feldspathic (fragments 30–120 μm in size), and basaltic compositions. Based on the chemical composition and appearance, the basaltic glasses are subdivided into two types. The glass of the first type has (50–200 μm in size) angular or rounded shape and contains vesicles, inclusions, and heterogeneities. The glasses of the second type occur as matrix glass or large fragments (70–300 μm), which are characterized by flow textures, heterogeneities, and contain numerous inclusions and vesicles. The wide diversity of lithic, mineral, and glassy clasts indicates a well-expressed polymictic composition of the breccia. Note that Dhofar 1442 has a high content of siderophile elements, the composition of which is consistent with metal of H-chondrites (Korotev, 2012). The detailed petrographic description of the rock can be found in the above-mentioned works.

The high content of incompatible elements (e.g., K, Th, U, REEs, P) in the meteorite and characteristic presence of the low-Ti basalts depleted in incompatible elements suggest that the rock was formed at the boundary of the highland rocks of Oceanus Procellarum (Procellarum KREEP Terrane) and mare basalts (Zeigler et al., 2011; Yang et al., 2019).

The U-Pb dating of the meteorite Dhofar 1442 revealed two age zircon groups: old (~4.3 Ga) and young (~3.9 Ga) (Zhou et al., 2012; Demidova et al., 2014), whereas phosphates have ages between ~3.2 and ~4.3 Ga with the main peak at ca. 3.8 Ga (Zhou et al., 2015). The correlation of petrographic composition of meteorite with zircon ages indicates that the KREEP magmatism in the source area of the meteorite Dhofar 1442 varied from mainly felsic to KREEP gabbro-norite within a period from 4.3 to 3.9 Ga, while the breccia was formed <3.8 Ga (Demidova et al., 2014).

EXPERIMENTAL TECHNIQUES

Since lunar breccias usually have a polymictic composition, it is reasonable to analyze separate clasts. However, this is frequently hampered by a limited amount of lunar meteorites and/or absence of technical facilities for local in situ analysis. At the same time, our previous works on the meteorites Dhofar 280 and Dhofar 1436 (Korochantseva et al., 2016b, 2021) showed that important geochronological and geochemical information can be also obtained for bulk samples of impact melt lunar breccias. This study was performed for a small bulk sample of the meteorite Dhofar 1442, which was divided into two roughly equal samples for analysis by stepwise combustion and crushing. The isotopic composition of noble gases, nitrogen and carbon in the bulk samples of the meteorite Dhofar 1442 was analyzed on the Finesse highly sensitive mass spectrometric complex (a single gas extraction and purification system coupled with three mass spectrometers operating in static mode) at the Open University (Milton Keynes, England; Wright et al., 1988; Wright and Pillinger, 1989; Verchovsky et al., 1998; Verchovsky, 2017).

One sample (7.25 mg) wrapped in a high-purity platinum foil was heated in an oxygen atmosphere in a double-walled quartz furnace within the temperature range from 200 to 1400°C with a step of 100°C (13 steps). The sample was hold at the temperature at each step for 30 min. After that, oxygen was sorbed back onto CuO before the gases released from the sample were sent to the separation and purification system. The second sample (7.50 mg) was studied by stepwise crushing with a cumulative number of strokes of 10300.

He and Ne were analyzed on a quadrupole mass spectrometer, while N_2 and Ar on a magnetic sector mass spectrometer. The carbon isotopic composition was measured on a separate magnetic sector mass spectrometer. The carbon (CO_2) amounts in the combustion and crushing steps were similar, but carbon isotopic composition could be measured in the sample during stepwise combustion only.

The purification procedure for gases released by stepwise crushing and combustion was identical to that described in (Korochantseva et al., 2020). The amount of the released carbon was measured from the CO_2 pressure using a MKS Baratron™ capacitance pressure gauge. Nitrogen and argon concentrations were analyzed by the peak height method using calibration with a known content of standard gases. The whole process of analysis on a Finesse complex is fully automated.

To reduce the contribution of doubly ionized masses (CO_2^{++} and $^{40}Ar^{++}$) to ^{20}Ne and ^{22}Ne, a low ionization voltage (~40 V) was used in the ion source of the quadrupole mass spectrometer. During the neon isotopic analysis, the static vacuum regime in mass-spectrometer camera was maintained with a Ti–Al getter.

The isotopic ratios are expressed in delta notation relative to standards (Vienna Peedee Belemnite (VPDB) for C and Earth's atmosphere (AIR) for N. The system blanks for stepwise combustion were determined before each sample measurement by analyzing empty clean platinum foil at the same temperatures as the sample. The blank values for stepwise combustion were ~2–6 ng for C, ~0.6 ng for N, ~2×10^{-7} cm^3 for ^{4}He, 0.3–7.5×10^{-10} cm^3 for ^{20}Ne, ~3×10^{-9} cm^3 for ^{40}Ar, and ~0.7×10^{-11} cm^3 for ^{36}Ar. The temperature dependence was observed only for C and Ne. The system blank during stepwise crushing was controlled several times: before crushing, after a step corresponding to over 1000 cumulative strokes on the sample, and at the end of the last crushing step by isolating the crushing system from vacuum pump for the time corresponding to the crushing duration at each step. The blank values at stepwise crushing were ~0.5 ng for C, ~0.25 ng for N, 1.8–2.5×10^{-8} cm^3 for ^{4}He, ~1×10^{-10} cm^3 for ^{20}Ne, ~3×10^{-9} cm^3 for ^{40}Ar, and ~1.3×10^{-11} cm^3 for ^{36}Ar. The dependence on the counting time was observed only for He.

The errors in the absolute gas concentrations are 5–10%, and those for noble gas elemental ratios are 5%.

RESULTS AND DISCUSSION

The results of the analyses of the light noble gases, carbon, and nitrogen obtained by the methods of stepwise combustion and crushing of the studied samples are given in Tables 1 and 2.

Kinetics of Gas Release

The majority of noble gases was released at temperatures above 600–700°C during stepwise combustion (Fig. 1a). This indicates that the amount of gases sorbed from the Earth's atmosphere is relatively low, i.e., gases are mainly of extraterrestrial origin. Helium is released slightly earlier and/or simultaneously with neon at 800–900°C, while the main peak of argon release is observed at temperature of 1100°C (Fig. 1b). The high-temperature (>1100°C) release of argon is also typical for the lunar impact melt breccias Dhofar 280 and Dhofar 1436 (Korochantseva et al., 2016b, 2021) and other types of impact metamorphosed meteorites (e.g., Kunz et al., 1997; Trieloff et al., 1994, 2018), which is likely related to a change of diffusion characteristics of argon in the mineral structures and K-bearing phases under influence of impact metamorphism. This can be exemplified by an increase of feldspar density at impact compression (Ahrens et al., 1969), which results in an increase of the activation energy of gas releases. Another example (Trieloff et al., 2018) is the formation of high-pressure jadeite after feldspar. As a result, the K–Ar system becomes more resistant to the thermal events. For comparison, argon degassing from K-bearing phases of meteorites that have not

Table 1. Noble gases (He, Ne and Ar), nitrogen and carbon, released during stepwise combustion from the lunar meteorite Dhofar 1442 (7.25 mg)

T, °C	$^{4}He \times 10^{-8}$	$^{20}Ne \times 10^{-8}$	$^{20}Ne/^{22}Ne$	$^{21}Ne/^{22}Ne$	$^{36}Ar \times 10^{-8}$	$^{40}Ar/^{36}Ar$	$^{36}Ar/^{38}Ar$	$^{4}He/^{20}Ne$	$^{20}Ne/^{36}Ar$	N, ppb	$\delta^{15}N$, ‰	C, ppm	$\delta^{13}C$, ‰
200	10778	n.a.	n.a.	n.a.	1.3	282(1)	5.24(6)	n.a.	n.a.	938	−11(4)	69.0	−26.2(1)
300	1125	0.6	n.a.	n.a.	6.3	139(1)	5.32(8)	1899.8	0.09	19459	6(3)	184.5	−25.4(3)
400	1036	0.5	n.a.	n.a.	2.1	300(1)	2.85(2)	2024.3	0.25	9799	5(3)	194.2	−21.3(2)
500	962	1.8	n.a.	n.a.	4.3	124(1)	3.56(1)	540.3	0.42	3312	3(3)	127.1	−14.8(2)
600	2305	15.7	9.80(70)	0.0413(72)	33.5	48.8(2)	n.a.	146.5	0.47	4830	3(3)	448.4	−0.1(2)
700	22357	128.2	10.20(20)	0.0408(39)	133.7	29.9(1)	5.29(1)	174.4	0.96	6624	6(3)	259.2	0.6(2)
800	115374	1035.1	10.60(10)	0.0325(17)	273.3	24.2(1)	4.98(1)	111.5	3.79	4002	11(3)	53.1	−1.9(2)
900	140767	2290.9	10.80(7)	0.0330(11)	342.3	21.5(1)	5.21(1)	61.4	6.69	1656	3(4)	14.8	−3.9(2)
1000	35468	897.0	10.10(7)	0.0426(12)	415.4	19.3(1)	n.a.	39.5	2.16	1104	11(4)	10.5	−4.7(3)
1100	2512	270.5	n.a.	n.a.	2842.9	14.1(1)	n.a.	9.3	0.10	9108	−5(3)	20.6	5.2(2)
1200	2967	33.3	n.a.	n.a.	94.8	25.2(1)	4.78(1)	89.2	0.35	731	n.a.	5.5	−16.5(3)
1300	7	8.2	n.a.	n.a.	0.4	129(9)	4.67(14)	0.9	19.10	83	−18(14)	0.7	−26.0(1.4)
1400	125	n.a.	n.a.	n.a.	n.a.	n.a.	n.a.	n.a.	n.a.	55	−30(20)	0.9	−25.4(1.3)
Total	335784	4682	10.58(8)	0.0352(14)	4150.3	17.5(1)	5.07(1)	71.7	1.13	61703	4(3)	1388.5	−9.1(2)

Contents of noble gases are given in cm^3 STP/g.
Numbers in parentheses refer to the last digits and are analytical uncertainties within 1σ.
Uncertainty of absolute concentrations of noble gases is 5–10%.
(n.a.) not analyzed.

Table 2. Noble gases (He, Ne and Ar), nitrogen and carbon released during stepwise crushing from the lunar meteorite Dhofar 1442 (7.50 mg)

Cumulative number of strokes	$^{4}He \times 10^{-8}$	$^{20}Ne \times 10^{-8}$	$^{20}Ne/^{22}Ne$	$^{21}Ne/^{22}Ne$	$^{36}Ar \times 10^{-8}$	$^{40}Ar/^{36}Ar$	$^{36}Ar/^{38}Ar$	$^{4}He/^{20}Ne$	$^{20}Ne/^{36}Ar$	N, ppb	$\delta^{15}N$, ‰	C, ppm	$^{14}N/^{36}Ar^{*}$	$^{12}C/^{36}Ar^{*}$
10	1907	57.6	10.51(11)	0.0300(32)	404.1	18.5(1)	5.53(2)	33.1	0.14	627	−13 (2)	0.3	96.5	38.6
30	1097	37.7	11.55(9)	0.0294(22)	149.2	17.3(1)	5.52(3)	29.1	0.25	133	−21(3)	0.4	55.6	161.3
70	3773	107.1	10.09(10)	0.0294(35)	199.9	16.8(1)	5.51(2)	35.2	0.54	200	−23(2)	0.6	62.3	184.3
150	4547	144.0	10.55(9)	0.0316(32)	147.8	17.4(1)	5.42(8)	31.6	0.97	267	−18 (2)	1.3	112.3	542.2
310	4867	169.3	10.54(9)	0.0308(28)	110.8	16.9(9)	5.51(3)	28.7	1.53	347	−11(2)	3.7	194.7	2059.4
630	4520	181.3	10.53(10)	0.0294(28)	56.6	17.2(2)	5.48(6)	24.9	3.20	640	−1(2)	10.8	703.6	11 901.9
1270	3867	180.0	10.26(8)	0.0313(26)	40.0	18.0(3)	5.43(7)	21.5	4.50	1213	4(1)	9.9	1888.5	15 335.9
2550	2027	101.3	10.76(24)	0.0309(29)	27.4	22.1(3)	5.35(10)	20.0	3.70	1880	9(1)**	13.0	4267.1	29 506.7
5110	861	69.3	11.34(6)	0.0357(16)	28.1	22.1(3)	5.24(15)	12.4	2.47	2947	15(1)	17.3	6524.4	38 378.8
10 300	475	46.7	11.86(11)	0.0346(19)	28.3	23.3(3)	5.27(9)	10.2	1.65	3520	19(1)	11.6	7731.2	25 448.4
Total	27940	1094.4	10.60(10)	0.0310(28)	1192.2	18.0(2)	5.49(4)	25.5	0.92	11 773	9(1)	68.8	614.5	3590.8

Contents of noble gases are given in cm^3 STP/g.

Numbers in parentheses refer to the last digits and are analytical uncertainties within 1σ.

Uncertainty of absolute concentrations of noble gases is 5–10%.

* Weight.

** Value obtained by interpolation.

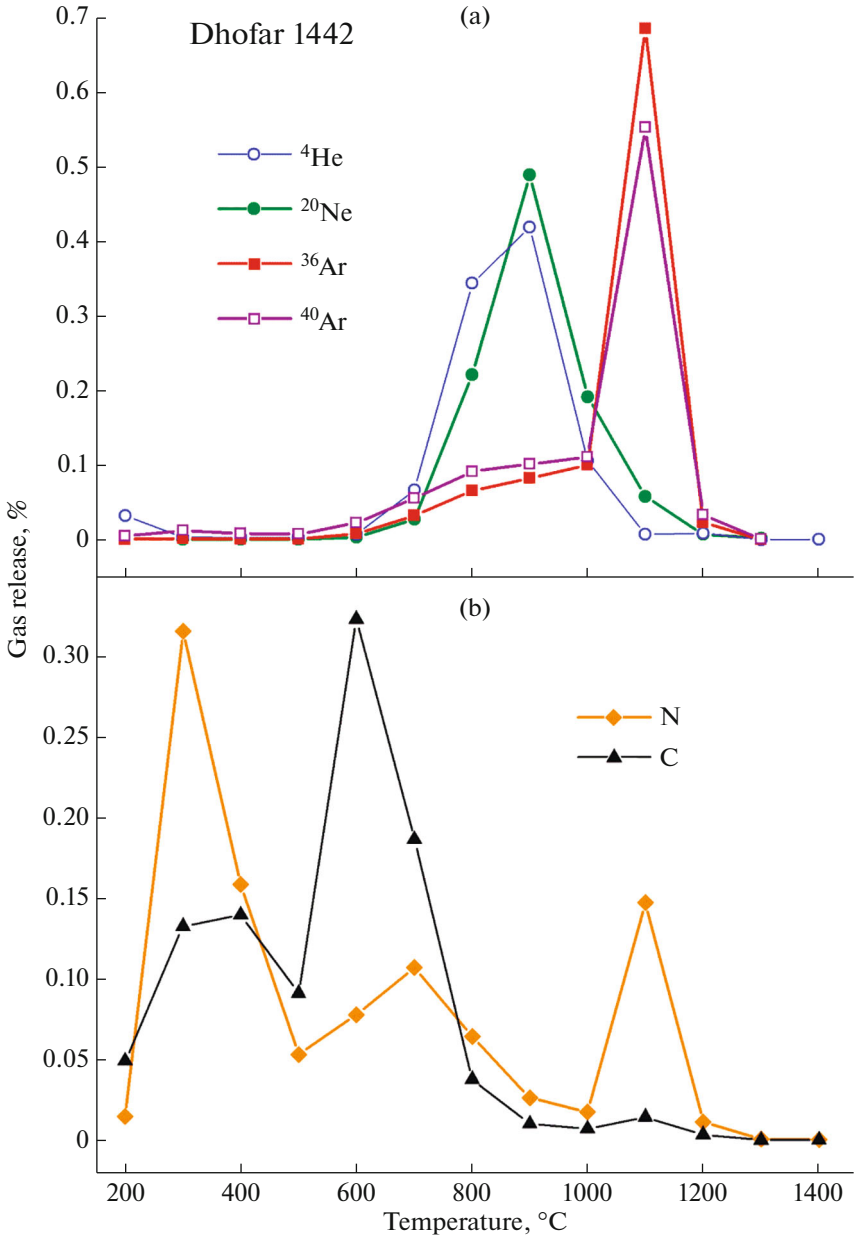

Fig. 1. Release kinetics of noble gases (a), nitrogen and carbon (b) during stepwise combustion of the bulk sample of the meteorite Dhofar 1442.

experienced a significant impact metamorphism occurs at temperature <1000°C (see Trieloff et al., 2003; 2018). Unlike noble gases, most of nitrogen and carbon are released at low temperatures, that is related to oxidation of organics, degassing of adsorbed atmospheric gases, and decomposition of carbonates formed through weathering when meteorite resided in desert after fall. It is noteworthy that the high-temperature nitrogen peak and the main peak of argon are released at the same temperature (1100°C), and a small peak of carbon release is also observed at this temperature. Similar pattern was observed also for the lunar meteorite Dhofar 1436: the high-temperature release of argon (1200–1300°C), in which the trapped lunar components are dominated, coincides with the peak of isotopically light nitrogen ($\delta^{15}N = -79‰$) which is mainly represented by nitrogen of solar origin, and with a small carbon peak (Korochantseva et al., 2021). A simultaneous degassing of these components was explained by the release of gases redistributed in the voids of different phases (minerals, glasses) after impact events. Note, this is related to melting of host phases rather than to decrepitation, as judged from the simultaneous release of argon isotopes formed on K and Ca in the rapid neutron flux at Ar–Ar dating. These argon isotopes are released from structure of K- and Ca-bearing phases (Korochantseva et al., 2021).

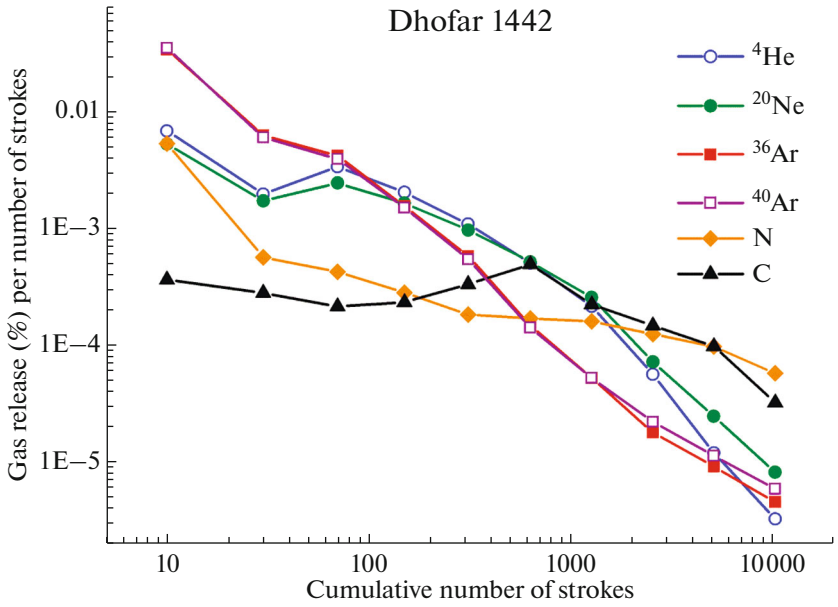

Fig. 2. Release patterns of volatile elements determined as the amount of gas (in %) released per a stroke during crushing of the lunar breccia sample Dhofar 1442.

A simultaneous release of ^{36}Ar, ^{40}Ar, and N is also observed in the lunar regolith samples returned by Luna missions 16 and 24 (Assonov et al., 2002). Authors of the cited work supposed that the source of trapped ^{40}Ar is re-implanted ^{40}Ar from lunar atmosphere. The latter is implanted in regolith grain with much lower energy (1–2 keV) than solar ^{36}Ar (30–36 keV) (Baur et al., 1972; Heymann and Kirsten, 1973; Manka and Michel, 1970), which should lead to a different implantation depth of these isotopes and different temperatures of their degassing. Based on these considerations Assonov et al. (2002) explained the simultaneous release of ^{40}Ar and ^{36}Ar by their redistribution and homogenization during reworking of regolith material, which is in line with the interpretation proposed above. However, it should be taken into account that re-implanted ^{40}Ar is not a single source of the trapped ^{40}Ar in lunar rocks. This was discussed in 1970s (Heymann et al., 1970; Manka and Michel, 1971; Baur et al., 1972) and described in detail later in (Korochantseva et al., 2021). Thus, as has been stated in the latter paper, not only re-implanted ^{40}Ar but all other Ar components accumulated in these soils could be involved in gas mobilization and redistribution.

Figure 2 demonstrates the release patterns of volatile elements (in %) normalised to the number of stroke. The release of all gases systematically (exept for helium, neon, and carbon) decreases with crushing (Fig. 2), that is typical for this kind of extraction (e.g., Korochantseva et al., 2018; Korochantseva et al., 2020). It is noteworthy that at the initial steps, when gases are released from the positions easyly accessible for crushing (mechanically instable phases and/or relatively large voids), the fraction of argon release is higher than those for other gases. In the following steps, the amount of the released argon relatively rapidly decreases with the number of strokes (argon line intersects all other lines in Fig. 2), while helium and neon release curves practically coincide with each other.

Content and Isotopic Composition of Noble Gases

Stepwise combustion and crushing yielded 3357.8 and 279.4 of ^{4}He; 46.8 and 10.9 of ^{20}Ne; 41.5 and 11.9 of ^{36}Ar ($\times 10^{-6}$ cm^3 STP/g), respectively. Crushing yielded 8, 23 and 29% of the total concentrations (obtained by stepped combustion) of ^{4}He, ^{20}Ne and ^{36}Ar, respectively. Note, however, that the percentages are not particularly precise since they were obtained for different sample aliquots of the polymictic breccia for which a certain heterogeneity is expected. It is correctly to calculate the percentages using gas concentrations in the powder remained after crushing that are not known for the Dhofar 1442 sample. For comparison, in the impact melt breccia Dhofar 1436 76–98% of their total ^{4}He, ^{20}Ne and ^{36}Ar are released during crushing (Korochantseva et al., 2021), though the gas concentrations in voids of the meteorite Dhofar 1442 are comparable with those of Dhofar 1436. However, the KREEP-rich meteorite Dhofar 1442 has much higher total ^{4}He concentrations, which can be related to the elevated Th and U concentrations in it. Obviously, practically all gases in Dhofar 1436 are located in the voids, that seems to be not the case for Dhofar 1442.

On the three-isotope neon diagram the data points are arranged along solar wind fractionation line (Fig. 3). The contribution of the cosmogenic component in the

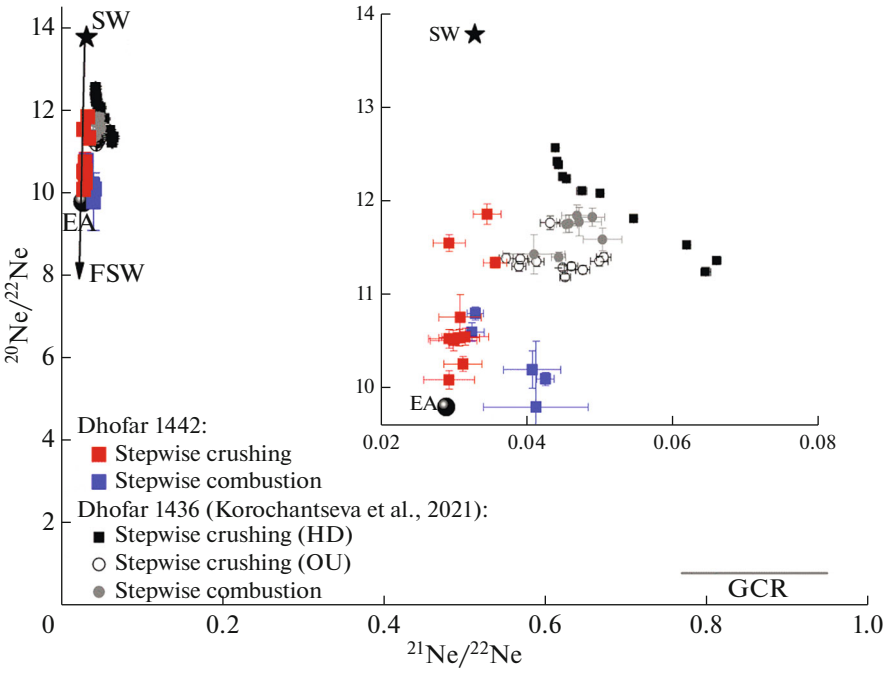

Fig. 3. Variations in the neon isotopic composition upon stepwise combustion and crushing of the meteorite Dhofar 1442 samples. The data on isotopic composition of neon extracted by the same methods from the bulk samples of the impact melt lunar breccia Dhofar 1436 (Korochantseva et al., 2021) are shown for comparison. Stepwise crushing of the Dhofar 1436 samples was performed at the Laboratory of the Heidelberg University, Germany (HD), and at the Laboratory of the Open University (OU), England. The compositions of the solar wind (SW; Heber et al., 2009), the Earth's atmosphere (EA; Eberhardt et al., 1965) and the range for the cosmogenic neon (Korochantseva et al., 2021) are also shown for reference. The composition of the solar wind fractionated Ne (FSW) is shown according to Grimberg et al. (2006).

polymictic breccia Dhofar 1442 is lower than in the Dhofar 1436 enriched in solar wind gases.

The variations of the $^{40}Ar/^{36}Ar$ ratio in the sample studied by stepwise crushing are relatively narrow compared to those in sample studied by stepwise combustion (Fig. 4; Tables 1, 2). This ratio varies within 17–19 in the first seven crushing steps, when most part of Ar is released, and increases to 22–23 in the last three steps. In the combustion experiment, the first steps have $^{40}Ar/^{36}Ar \sim 300$, which indicates a contamination by atmospheric argon. In the following steps, the $^{40}Ar/^{36}Ar$ ratio gradually decreases and reaches minimum values of 14–22 at 900–1100°C, which correspond to the main peak of argon release (at maximum, the $^{40}Ar/^{36}Ar$ ratio reaches the lowest value of 14). These values almost coincide with those during crushing. Hence, the lunar argon with $^{40}Ar/^{36}Ar \sim 18$ was trapped in the voids of the high-temperature phases. Such conclusion has also been made for other meteorites that had been altered by impact metamorphism and studied by methods of stepwise crushing, combustion, and pyrolysis (Korochantseva et al., 2018, 2021). Similar inference was made by Japanese researchers (Takaoka et al., 1996), who suggested that the gases released by crushing from an enstatite chondrite have been trapped in microbubbles during impact melting. Korochantseva et al. (2018, 2021) relate the origin of trapped gases in chondrite breccias to mobilisation of solar, cosmogenic, and radiogenic noble gases, as well as re-implanted ^{40}Ar, which have been accumulated in the material prior to the impact events in lunar samples and then partly redistributed from one structural sites into others, in particular, into voids, from which they can be extracted by crushing. Korochantseva et al. (2021) proposed that voids could be formed by sintering and agglutination along grain boundaries owing to the thermal events that accompanied the impact cratering. It should also be noted that the isotopic composition of trapped argon in Dhofar 1442 with $^{40}Ar/^{36}Ar \sim 18$ is inconsistent with the empirical model, which relates the presence of ^{40}Ar in the regolith only to its implantation from the lunar atmosphere (McKay et al., 1986; Eugster et al., 2001; Joy et al., 2011). According to the model, at the age of the Dhofar 1442 < 3.8 Ga (Demidova et al., 2014) the corresponding $(^{40}Ar/^{36}Ar)_{trap}$ is < 15. The extraterrestrial trapped argon has been already identified in lunar meteorites and Apollo mission regolith samples with $^{40}Ar/^{36}Ar$ ratios higher than required by the model mentioned above (Huneke et al., 1973; Bogard et al., 1975; Schaeffer and Schaeffer, 1977; Korochantseva et al., 2016 b, c). Other inconsistencies of the model are reported in (Korochantseva et al., 2016b, 2021).

The $^{36}Ar/^{38}Ar$ ratio in the crushing steps is more than 5.24, which indicates a high fraction of trapped Ar component and relatively low contribution of cos-

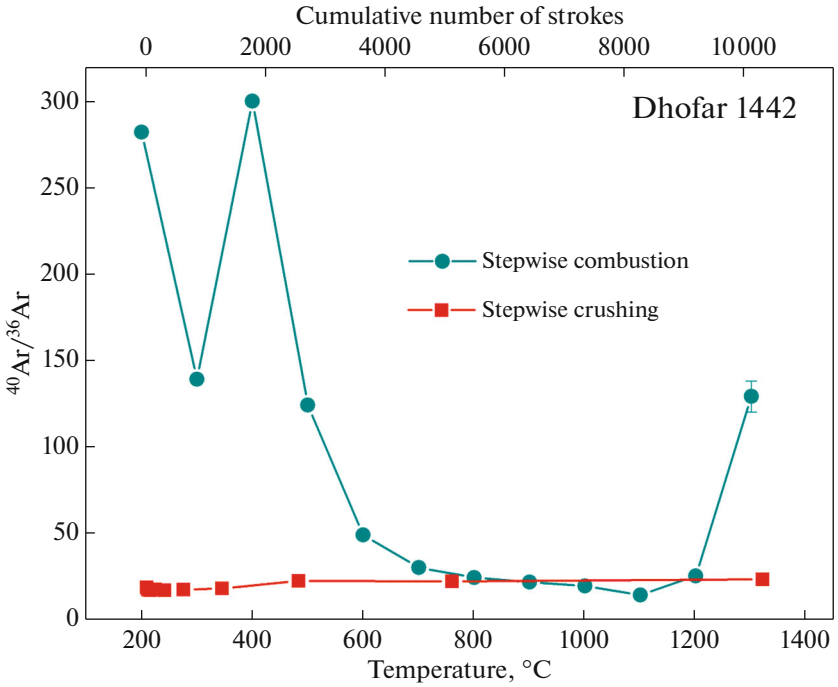

Fig. 4. Variations of the $^{40}Ar/^{36}Ar$ ratio during stepwise combustion and crushing of the Dhofar 1442 samples.

mogenic component in Dhofar 1442. In other meteorites, where contribution of cosmogenic Ar is higher than in Dhofar 1442, the $^{36}Ar/^{38}Ar$ ratio tends to decrease with progressive crushing, thus showing an increase of cosmogenic component contribution, (Buikin et al., 2013, 2015; Korochantseva et al., 2018, 2021). Similar is observed during heating and etching (e.g., Wieler et al., 1986; Eugster et al., 1992, 1996).

Carbon and Nitrogen

The obtained data for carbon and nitrogen described in this chapter are repeatedly compared with those obtained for the lunar meteorite Dhofar 1436 (Korochantseva et al., 2021). Therefore, hereafter, when mentioning the Dhofar 1436 breccia the reference to this article is automatically implied.

The concentration of nitrogen (12 ppm) released during crushing is ~20% of the total nitrogen content (62 ppm). Approximately the same proportion (~15%) is determined for nitrogen released from the breccia Dhofar 1436. The carbon content (69 ppm) released at crushing is near 5% of that extracted by combustion (1388 ppm). Thus, the fraction of the chemically bound carbon is higher than that for the chemically bound nitrogen. The main releases of nitrogen and carbon occur at low temperatures, which is mainly related to the terrestrial contamination. At 900–1400°C, when extraterrestrial nitrogen, carbon and most of argon are simultaneously released (Figs. 1a, 1b), the amounts of the released nitrogen and carbon (20.6 and 3.8%, correspondingly) are comparable with the total release of the gases during stepwise crushing. The C/N ratio in gases released by combustion at 900–1300°C is 2.3–9.5 (Fig. 5). Most crushing steps shows the same range of the C/N ratio. The gases released by crushing have the bulk C/N = 5.8. Such low C/N ratios are closer to the solar values (Anders and Grevesse, 1989) than to the values typical for the organics in metamorphosed chondrites (~30, Alexander et al., 2007). As mentioned above, the high-temperature release of the gases is associated with voids. Similarity of the C/N ratios observed during crushing and the high-temperature combustion is an additional argument for that. We may suggest that significant amount of nitrogen and carbon presented in the rocks prior to the impact event have been redistributed into the voids as a result of the event. It is noteworthy that the gas released at 1200–1460°C from the solar gas-rich Dhofar 1436 meteorite demonstrate the same ratio C/N = 4–9. In addition, these values are comparable with values reported for lunar regolith samples (Assonov et al., 2002), as well as lunar basalts and enstatite chondrites (Mortimer et al., 2015, references therein). The gases trapped in the meteorite Dhofar 1442 could involve not only solar gases, but also nitrogen and carbon formed through oxidation of the organics of metamorphosed chondrites, which are present in the breccia (Korotev, 2012), for instance by interaction of the organics with the oxygen-bearing minerals.

In the combustion steps, $\delta^{13}C$ varies from –26.2 to 5.2‰ with a bulk value of –9.1‰ (Fig. 6, Table 1). The same range of variations of carbon isotopic composition was obtained for the lunar breccia Dhofar 1436 (–28...+11‰), although carbon in this meteorite has a lighter bulk isotopic composition ($\delta^{13}C$ = –15.8‰)

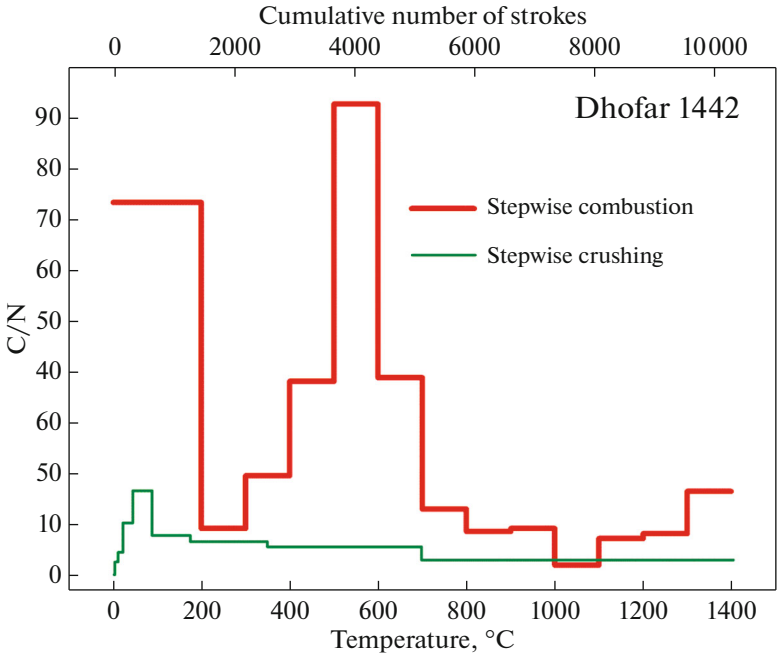

Fig. 5. Variations of the C/N ratio (wt) during stepwise combustion and crushing in the Dhofar 1442 samples.

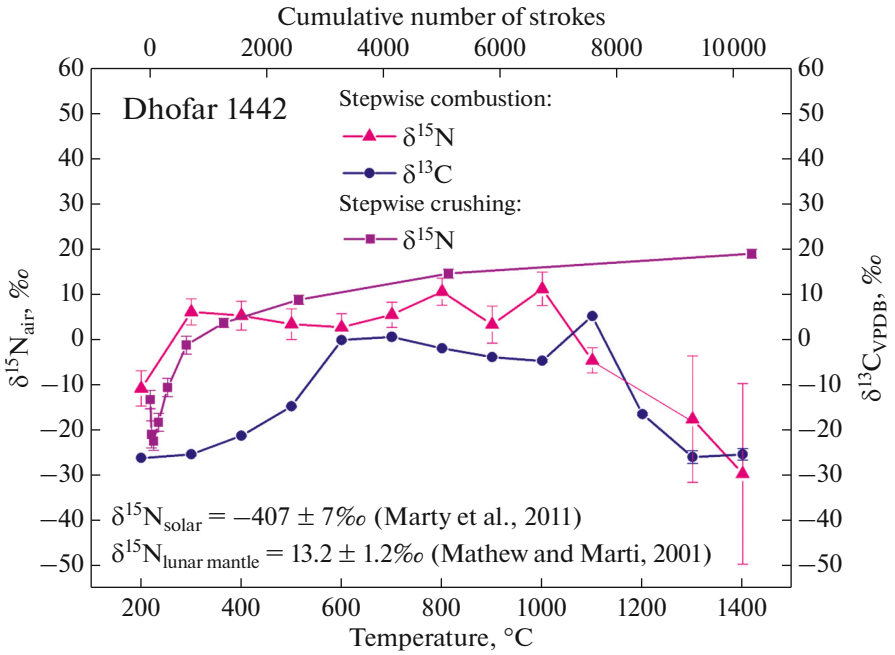

Fig. 6. Variations of the nitrogen and carbon isotope composition upon stepwise combustion and crushing in the samples of the lunar breccia Dhofar 1442.

than that observed in Dhofar 1442. In addition, both meteorites show similar "two-humped" $\delta^{13}C$ variations depending on temperature, while carbon with the isotopically heaviest composition is released at temperature of the main release of trapped argon and the high-temperature peak of nitrogen.

The isotopic composition of nitrogen released by stepwise combustion from the meteorite Dhofar 1442 varies from −30 to +11‰ with bulk composition of +4‰ (Fig. 6; Table 1). The nitrogen isotopic composition of Dhofar 1442 meteorite is much heavier than that of the impact melt breccia Dhofar 1436 ($\delta^{15}N_{bulk}$ = −25.3‰ at stepwise combustion and $\delta^{15}N_{bulk}$ = −28.4‰ at stepwise crushing). Taking into account that the fraction of cosmogenic noble gases (Ne, Ar) in the Dhofar 1442 sample is very low, the heavier nitrogen

isotopic composition of the regolith breccia Dhofar 1442 compared to that of Dhofar 1436 is related to a contribution of nitrogen from the chondritic impactors ($\delta^{15}N_{ordinary\ chondrite}$ is within −20 to +100 after Grady and Wright, 2003), the material of which is present in Dhofar 1442 (see above "Meteorite Description"), and/or to the lower amount of solar gases, which would also explain the heavier carbon isotopic composition. In the lunar breccia Dhofar 1442, after the first crushing step likely contaminated by atmospheric/organic nitrogen, the $\delta^{15}N$ value increases from step to step from −23 to +19‰ (Fig. 6, Table 2). This is hardly related to the increasing contribution of the isotopically heavy cosmogenic nitrogen, because this tendency is not observed for noble gases. The more probable explanation is the decrease of the contribution of the trapped component during stepwise crushing, when the sizes of the destroyed voids decrease with each successive step. The bulk value $\delta^{15}N = +9‰$ obtained at stepwise crushing of Dhofar 1442 is close to that observed during stepwise combustion. The same relationship in nitrogen isotopic composition is observed for Dhofar 1436 (see above), although its $\delta^{15}N$ values are lower than those in Dhofar 1442. This could mean that the isotopic composition of nitrogen trapped in the voids of Dhofar 1442 on average corresponds to that of the chemically bound nitrogen and could be regarded as a confirmation of the origin of the former through the redistribution of the latter in the void during post-impact period. However, most of nitrogen released during combustion of Dhofar 1442 is related to the terrestrial contamination. Therefore, the coincidence of the bulk isotopic compositions of nitrogen evolved during combustion and crushing is likely accidental. Finally, we have to note that since most of carbon and nitrogen in Dhofar 1442 is not of solar origin the close to solar C/N ratio in the sample is obviously due to element fractionation associated with the redistribution process.

Elemental Ratios

The elemental ratios of noble gases obtained by stepwise crushing of the lunar meteorite Dhofar 1442 sample are highly fractionated relative to those of solar wind (Heber et al., 2009; Table 2). The fractionation was mainly caused by the impact events and subsequent post-impact processes, which led to the transition of previously accumulated gases into voids: most part of the light gases was lost from the rock into surrounding space, whereupon the remained gases already enriched in the heavy component were partly trapped in the voids. However, diffusion losses of light isotopes relative to heavy ones from the material in response to its multiple heating by the impact events and/or solar radiation could occur during entire lunar evolution of the material: prior to and after this event. Although the most obvious and efficient mechanisms of gas release from voids are decrepitation and/or melting of their host, and, to much lesser extent, gas dissolution in solid matter with subsequent diffusion, it is impossible to exclude a direct diffusion of the gases from voids, as it follows from the data for the Dhofar 1436 lunar meteorite. Crushing of the Dhofar 1436 sample results in degassing of 93% ^{4}He, 86% ^{20}Ne, and 76% ^{36}Ar of their total amounts (Korochantseva et al., 2021), i.e., gases in this meteorite are mainly located in voids. It was also shown in the cited work that combustion of the Dhofar 1436 bulk sample yielded a peak of helium release at 900°C, and peaks of neon and argon at 1200–1300°C, when host phases are melted (see above). The earlier release of helium from the voids is likely caused by its higher solubility and diffusivity in solids compared to neon and argon. The presence of the cosmogenic component with much lower He/Ne and He/Ar ratios relative to solar hardly affects the elemental abundance of noble gases in Dhofar 1442. The influence of the planetary components is possible to some extent.

The $^{4}He/^{20}Ne$ ratio at the initial crushing steps is approximately constant, and then decreases by ~ 3 times in the following crushing steps, with the most sharp decreasing only in the two last steps, which however contain insignificant amount of the total He and Ne (Table 2). The lunar breccia Dhofar 1436 and L-chondrite breccia Ghubara show an opposite tendency, which cannot be explained by the presence of the radiogenic or cosmogenic ^{4}He at the late crushing stages, but rather expresses different elemental abundance of gases in the voids of various sizes (Korochantseva et al., 2018, 2021), which is also likely the case for Dhofar 1442. In addition, given the higher permeability of helium compared to other noble gases, the decrease of $^{4}He/^{20}Ne$ ratio during crushing can be explained by the following reasons: (i) the fraction of gases diffused out from the voids increases with decreasing the void radius (i.e., it is proportional $1/R$, where R is the radius), since, all other things being equal, the losses are proportional to the surface area, while the amount of gas in the voids is proportional to their volume (R^3); (ii) although the effective temperature of the sample during crushing does not exceed 70°C (Moreira and Madureira, 2005), it could significantly be increased locally due to collision of grains and thus facilitate helium escape from voids (see above); in addition, newly formed fractures significantly simplifies He earlier release from the rock compared to the larger gas atoms.

The $^{4}He/^{36}Ar$ and $^{20}Ne/^{36}Ar$ ratios permanently increase (by factors of 20 and 32 respectively, which is much more significant than the decrease of the $^{4}He/^{20}Ne$ ratio) in the first seven steps, and only three last steps show an opposite trend (Fig. 7; Table 2). The $^{14}N/^{36}Ar$ and $^{12}C/^{36}Ar$ ratios also rapidly increase with crushing: by factors of ~100 and ~1000, respectively (Fig. 8, Table 2). The excess argon in the first crushing steps cannot be explained by the atmospheric contam-

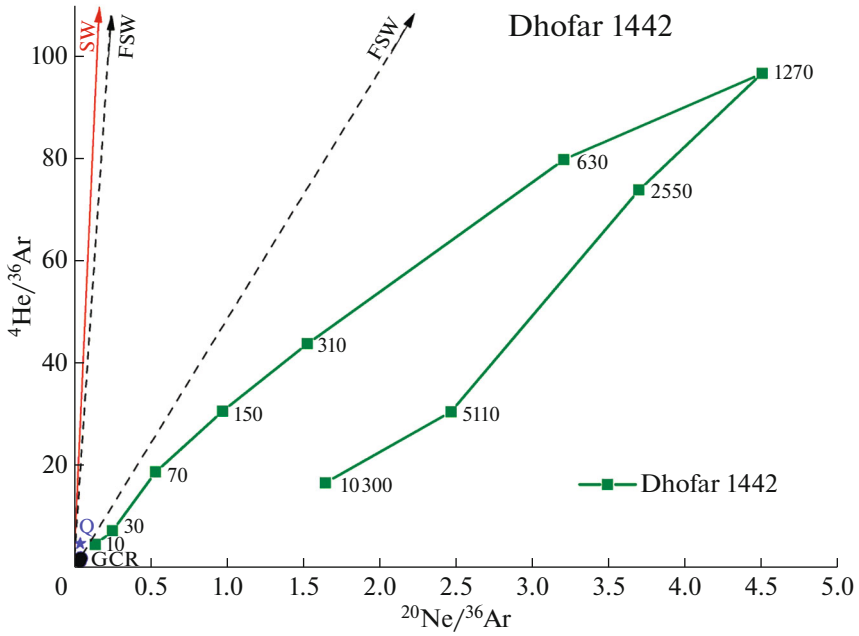

Fig. 7. The $^{20}Ne/^{36}Ar$–$^{4}He/^{36}Ar$ diagram for the stepwise crushing data of the lunar breccia Dhofar 1442 sample. The following compositions are shown for reference: Solar wind (SW; Heber et al., 2009), fractionated solar wind (FSW; Benkert et al., 1993), planetary component (Q; Ott, 2002), and cosmogenic component (GCR) forming under the influence of galactic cosmic rays (isotope composition was calculated for the chemical composition of the Dhofar 1442 and meteoroid with radius of 150 cm, with allowance for different shielding depth according to the model of Leya and Masarik, 2009).

ination, since the $^{40}Ar/^{36}Ar$ ratio in these steps is within 17–19 (Fig. 4; Table 2), although the isotopic composition of nitrogen in the same initial step implies an admixture of atmospheric/organic nitrogen (see section "Carbon and nitrogen", Fig. 6). An increase of the $^{4}He/^{36}Ar$ and $^{20}Ne/^{36}Ar$ ratios, in the course of crushing was also observed in the Dhofar 1436 lunar meteorite (Fig. 10 in Korochantseva et al., 2021) and was explained by the increasing contribution of cosmogenic component. However, in the case of Dhofar 1442, the reason must be different. Apart from very low, if any, contribution of the cosmogenic component, the mentioned above observations that the fraction of the released argon in the first crushing steps is higher than that for other gases, and the kinetics of helium and neon release is not correlated with the kinetics of argon release (Fig. 2) may also play a role.

Wide variations of the $^{4}He/^{36}Ar$, $^{20}Ne/^{36}Ar$, $^{14}N/^{36}Ar$, and $^{12}C/^{36}Ar$ ratios reflect an extremely uneven distribution of gases between voids of different sizes. Argon is mainly located in the large voids, the helium and neon—in the medium voids, while carbon and especially nitrogen are mainly associated with small voids. A possible scenario, which could explain the observations, suggests a combination of a complex dynamics of release and redistribution of the gases from different sources along with an equally complex dynamics of the formation of the voids during impact metamorphism. The uneven distribution of gases in the voids implies that different gases were differently mobilized during impact processes rather than were released simultaneously from their carrier phases, creating thus an intermediate homogenous atmosphere, which was trapped in all voids. Ar showing the invariable $^{40}Ar/^{36}Ar$ ratio in all crushing steps is likely the most mobile gas or even occurred in large voids prior to impact where retained. This was followed by the mobilisation of solar He and Ne, and, finally, carbon and nitrogen. In addition, the voids of different sizes were likely formed not simultaneously (as well as the gas release) but successively, from larger to smaller ones. The redistribution likely occurred rapidly, within a short time interval, but after that has continued for some time until temperature has remained high enough for diffusion. Thus, we believe that the uneven distribution of gases in voids, which result in a strong increase of the $^{4}He/^{36}Ar$, $^{20}Ne/^{36}Ar$, $^{14}N/^{36}Ar$, and $^{12}C/^{36}Ar$ ratios during crushing, is related to the dynamics of different processes during redistribution of the gases from different sources/positions in voids of various sizes during impact metamorphism.

CONCLUSIONS

In the lunar regolith breccia Dhofar 1442 found in the desert and having a porous matrix, noble gases are released mainly at ≥800°C, i.e., they are dominated by gases of extraterrestrial origin. Thereby, the crushing results indicate that significant fraction of the noble gases in this breccia is located in voids. Dhofar 1442 is characterized by the high-temperature (>1100°C) release of argon, which is typical of impact metamor-

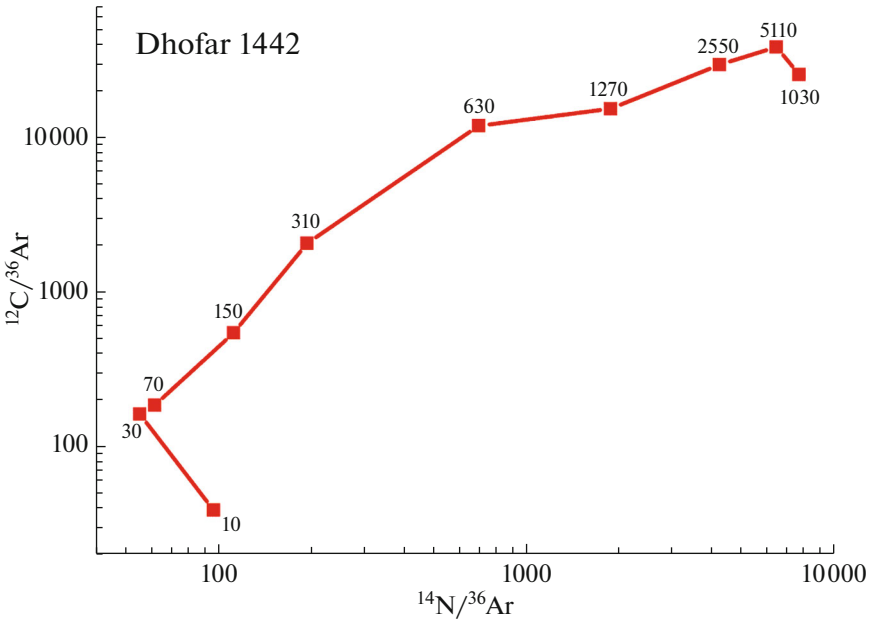

Fig. 8. The $^{12}C/^{36}Ar$–$^{14}N/^{36}Ar$ (wt) diagram for the stepwise crushing data of the lunar breccia Dhofar 1442 sample. Cumulative number of strokes is shown next to the data points.

phosed meteorites (Kunz et al., 1997; Trieloff et al., 1994, 2018; Korochantseva et al., 2016b, 2021), in which the solid phases experienced structural transformations. Simultaneous high-temperature degassing of argon, nitrogen, and carbon trapped in the voids of the high-temperature phases is caused by melting of the latters.

The isotopic composition of neon corresponds to the composition of the fractionated solar wind. At stepwise crushing, the $^{20}Ne/^{22}Ne$ ratio in the gas released from voids is higher than 10. In the studied samples, the contribution of cosmogenic component to the isotopic composition of neon is insignificant, as in the case of argon.

Crushing and combustion results demonstrate that lunar argon trapped in the gas voids of the high-temperature phases has $^{40}Ar/^{36}Ar$ ~18. Given the age of Dhofar 1442 (<3.8 Ga according to Demidova et al. (2014)), this isotopic composition of trapped argon is inconsistent with the empirical model suggesting that ^{40}Ar was re-implanted from the lunar atmosphere (McKay et al., 1986; Eugster et al., 2001; Joy et al., 2011). We believe that argon and other volatile elements present in the voids of the breccia Dhofar 1442 resulted mostly from gas redistribution (which is accompanied by their significant fractionation) from one structural sites into others during thermal/impact events, in particular, during the breccia formation, rather than be only associated with implantation from the lunar atmosphere. In addition to solar, cosmogenic, radiogenic gases, and re-implanted ^{40}Ar, the meteorite Dhofar 1442 also contains nitrogen and carbon formed through the oxidation of organics of metamorphosed chondrites, which are present in the breccia (Korotev, 2012).

The isotopic compositions of carbon ($\delta^{13}C$) and nitrogen ($\delta^{15}N$) released by stepwise combustion from the meteorite Dhofar 1442 sample vary from −26.2 to +5.2‰ and from −30 to +11‰, respectively. The $\delta^{15}N$ at stepwise crushing varies from −23 to +19‰. The bulk values of $\delta^{15}N$ during stepwise combustion and crushing are close to each other. This indicates that the isotopic composition of nitrogen localized in voids on average corresponds to the isotopic composition of the chemically bound nitrogen, thus likely indicating the origin of the former through the redistribution of the latter in voids during post-impact period. Although, the coincidence of the bulk values could be occasional, because most of nitrogen released during combustion is related to the terrestrial contamination.

Crushing is accompanied by variations of the elemental ratios. A slight decrease of the $^{4}He/^{20}Ne$ ratio during crushing could reflect the distribution of these gases into the voids of different sizes and/or be related to differences in the diffusion properties and permeability of helium and neon, which occur both in natural thermal processes and during laboratory heating. The $^{4}He/^{36}Ar$, $^{20}Ne/^{36}Ar$, $^{14}N/^{36}Ar$, and $^{12}C/^{36}Ar$ ratios show an opposite trend, increasing by tens to hundreds times during crushing. This is related to the fact that the fraction of argon in the positions most accessible for crushing is higher than that of other gases, while the argon release pattern differs from those of helium and neon. Such strong increase of elemental ratios during crushing of the meteorite Dhofar 1442 sample can be caused by specific combination of dynamically different processes that accompany the redistribution of gases from different positions/sources into the voids of various sizes during impact metamorphism, and

resulted in the uneven distribution of the volatile elements and argon fractionation relative to other gases.

ACKNOWLEDGMENTS

We are grateful to A.I. Buikin for fruitful discussion. Reviewers A.T. Bazilevsky and S.S. Assonov are thanked for comments, which significantly improved the manuscript.

FUNDING

This work was made in the framework of government-financed task of GEOKHI RAS.

CONFLICT OF INTEREST

The authors declare that they have no conflicts of interest.

REFERENCES

T. J. Ahrens, C. F. Petersen, and J. T. Rosenberg, "Shock compression of feldspars," J. Geophys. Res. **74** (10), 2727–2746 (1969).

C. M. O'D. Alexander, M. Fogel, H. Yabita, and G. D. Cody, "The origin and evolution of chondrites recorded in the elemental and isotopic compositions of their macromolecular organic matter," Geochim. Cosmochim. Acta **71**, 4380–4403 (2007).

E. Anders and N. Grevesse, "Abundance of the elements: Meteoritic and solar," Geochim. Cosmochim. Acta **53**, 197–214 (1989).

S. S. Assonov, I. A. Franchi, C. T. Pillinger, C. S. Semenova, Yu. A. Shukolyukov, A. B. Verchovsky, and A. N. Iassevitch, "Nitrogen and argon release profiles in Luna 16 and Luna 24 regolith samples: The effects of regolith reworking," Meteorit. Planet. Sci. **37** (1), 27–48 (2002).

J. -P. Benkert, H. Baur, P. Signer, and R. Wieler, "He, Ne, and Ar from the solar wind and solar energetic particles in lunar ilmenites and pyroxenes," J. Geophys. Res. **98** (E7), 13147–13162 (1993).

D. D. Bogard, L. E. Nyquist, B. M. Bansal, H. Wiesmann, and C. Y. Shih, "76535: An old lunar rock," Earth Planet. Sci. Lett. **26**, 69–80 (1975).

A. I. Buikin, A. B. Verchovsky, C. A. Lorenz, A. Ya. Skripnik, and E. V. Korochantseva, "Noble gases and nitrogen released by crushing from Pesyanoe aubrite," *44th Lunar and Planetary Science Conference,* abstract #1141 (2013).

A. I. Buikin, J. Hopp, C. A. Lorenz, and M. Trieloff, "Noble gas isotope composition and elemental ratios in Pesyanoe aubrite: Stepwise crushing data," Meteorit. Planet. Sci. **50**, #5110 (2015).

S. I. Demidova, M. A. Nazarov, M. O. Anosova, Y. A. Kostitsyn, F. Brandstätter, and Th. Ntaflos, "U–Pb dating of zircons from the Dhofar 1442 lunar meteorite," *43rd Lunar and Planetary Science Conference,* abstract #1090 (2012).

S. I. Demidova, M. A. Nazarov, M. O. Anosova, Yu. A. Kostitsyn, Th. Ntaflos, and F. Brandstätter, "U-Pb zircon dating of the lunar meteorite Dhofar 1442," Petrology **22** (1), 1–16 (2014).

P. Eberhardt, O. Eugster, and K. Marti, "A redetermination of the isotopic composition of atmospheric neon," Z. Naturforsch. **20a**, 623–624 (1965).

O. Eugster, Th. Michel, and S. Niedermann, "Solar wind and cosmic ray exposure history of lunar meteorite Yamato-793274," *Proceedings of the National Institute for Polar Research Symposium on Antarctic Meteorites*, **5**, 23–35 (1992).

O. Eugster, Ch. Thalmann, A. Albrecht, G. F. Herzog, J. S. Delaney, J. Klein, and R. Middleton, "Exposure history of glass and breccia phases of lunar meteorite EET87521," Meteorit. Planet. Sci. **31** (2), 299–304 (1996).

O. Eugster, D. Terribilini, E. Polnau, and J. Kramers, "The antiquity indicator argon-40/argon-36 for lunar surface samples calibrated by uranium-235-xenon-136 dating," Meteorit. Planet. Sci. **36** (8), 1097–1115 (2001).

M. M. Grady and I. P. Wright, "Elemental and isotopic abundances of carbon and nitrogen in meteorites," Space Sci. Rev. **106** (1), 231–248 (2003).

A. Grimberg, H. Baur, P. Bochsler, F. Bühler, D. S. Burnett, C. C. Hays, V. S. Heber, A. J. G. Jurewicz, and R. Wieler, "Solar wind neon from Genesis: Implications for the lunar noble gas record," Science **314** (5802), 1133–1135 (2006).

V. S. Heber, R. Wieler, H. Baur, C. Olinger, T. A. Friedmann, and D. S. Burnett, "Noble gas composition of the solar wind as collected by the Genesis mission," Geochim. Cosmochim. Acta **73** (24), 7414–7432 (2009).

J. C. Huneke, F. A. Podosek, and G. J. Wasrburg, "An argon bouillabaisse including ages from the Luna 20 site," *4th Lunar and Planetary Science*, 403–405 (1973).

K. H. Joy, D. A. Kring, D. D. Bogard, D. S. McKay, and M. E. Zolensky, "Re-examination of the formation ages of the Apollo 16 regolith breccias," Geochim. Cosmochim. Acta **75** (22), 7208–7225 (2011).

E. V. Korochantseva, A. I. Buikin, J. Hopp, A. V. Korochantsev, and M. Trieloff, "^{40}Ar–^{39}Ar results of lunar meteorites Dhofar 025, 280, 309, 730, 733, 1436, 1442, SAU 449, NWA 6888," Meteorit. Planet. Sci. **51**, abstract #6317 (2016a).

E. V. Korochantseva, A. I. Buikin, J. Hopp, C. A. Lorenz, A. V. Korochantsev, U. Ott, and M. Trieloff, "Thermal and irradiation history of lunar meteorite Dhofar 280," Meteorit. Planet. Sci. **51** (12), 2334–2346 (2016b).

E. V. Korochantseva, A. I. Buikin, J. Hopp, A. V. Korochantsev, and M. Trieloff, "^{40}Ar–^{39}Ar dating of lunar meteorites Dhofar 309 and 730," *47th Lunar and Planetary Science Conference,* abstract #2305 (2016c).

E. V. Korochantseva, A. I. Buikin, A. B. Verchovsky, C. A. Lorenz, and A. V. Korochantsev, "Noble gases, nitrogen and carbon isotopic compositions of the Ghubara meteorite, revealed by stepwise combustion and crushing methods," Geochem. Int. **56** (13), 1384–1397 (2018).

E. V. Korochantseva, A. I. Buikin, A. B. Verchovsky, C. A. Lorenz, and A. V. Korochantsev, "Isotopic composition of noble gases, nitrogen, and carbon in the Ozerki new L chondrite," Geochem. Int. **58** (11), 1239–1256 (2020).

E. V. Korochantseva, A. I. Buikin, J. Hopp, A. B. Verchovsky, A. V. Korochantsev, M. Anand, and M. Trieloff, "The lunar Dhofar 1436 meteorite: ^{40}Ar–^{39}Ar chronology and volatiles, revealed by stepwise combustion and crushing methods," Meteorit. Planet. Sci. **56** (3), 455–481 (2021).

R. L. Korotev, "Lunar meteorites from Oman," Meteorit. Planet. Sci. **47** (8), 1365–1402 (2012).

R. L. Korotev, *Lunar Meteorite Compendium*, https://curator.jsc.nasa.gov/antmet/lmc/ Accessed 25 January, 2022 (2022a).

R. L. Korotev, "List of lunar meteorites. http://meteorites.wustl.edu/lunar/moon_meteorites_list_alumina.htm Accessed 25 January, 2022 (2022b).

R. L. Korotev, R. A. Zeigler, B. L. Jolliff, A. J. Irving, and T. E. Bunch, "Compositional and lithological diversity among brecciated lunar meteorites of intermediate iron concentration," Meteorit. Planet. Sci. **44** (9), 1287–1322 (2009).

J. Kunz, M. Falter, and E. Jessberger, "Shocked meteorites: Argon-40-argon-39 evidence for multiple impacts," Meteorit. Planet. Sci. **32**, 647–670 (1997).

I. Leya and J. Masarik, "Cosmogenic nuclides in stony meteorites revisited," Meteorit. Planet. Sci. **44** (7), 1061–1086 (2009).

B. Marty, M. Chaussidon, R. C. Wiens, A. J.G. Jurewicz, and D. S. Burnett, "A ^{15}N-poor isotopic composition for the solar system as shown by Genesis solar wind samples," Science **332** (6037), 1533–1536 (2011).

D. S. McKay, D. D. Bogard, R. V. Morris, R. L. Korotev, P. Johnson, and S. J. Wentworth, "Apollo 16 regolith breccias: Characterization and evidence for early formation in the mega-regolith," J. Geophys. Res. **91**, D277–D303 (1986).

M. Moreira and P. Madureira, "Cosmogenic helium and neon in 11 Myr old ultramafic xenoliths: Consequences for mantle signatures in old samples," Geochem., Geophys., Geosyst. **6**, https://doi.org/10 (2005).1029/2005GC000939

J. Mortimer, A. B. Verchovsky, M. Anand, I. Gilmour, and C. T. Pillinger, "Simultaneous analysis of abundance and isotopic composition of nitrogen, carbon, and noble gases in lunar basalts: Insights into interior and surface processes on the Moon," Icarus **255**, 3–17 (2015).

G. A. Schaeffer and O. A. Schaeffer, "^{39}Ar–^{40}Ar ages of lunar rocks, *Proceedings of the Eight Lunar Science Conference*, 2253–2300 (1977).

D. Stöffler, H. -D. Knöll, U. B. Marvin, C. H. Simonds, and P. H. Warren, "Recommended classification and nomenclature of lunar highlands rocks–A committee report," In *Proceedings of the Conference on the Lunar Highlands Crust*, Ed. by R. B. Merrill and J. J. Papike, (Lunar and Planetary Institute, Houston, 1980), pp. 51–70 (1980).

N. Takaoka, T. Nakamura, and K. Nagao, "A possible site trapping noble gases in Happy Canyon enstatite chondrite: Microbubbles," *21st Symposium on Antarctic Meteorites,* 167–169 (1996).

M. Trieloff, A. Deutsch, J. Kunz, and E. K. Jessberger, "Redistribution of potassium and radiogenic argon by moderate shock pressures in experimentally shocked gabbro," Meteoritics **29** (4), 541 (1994).

M. Trieloff, E. K. Jessberger, I. Herrwerth, J. Hopp, C. Fiéni, M. Ghélis, M. Bourot-Denise, and P. Pellas, "Structure and thermal history of the H-chondrite parent asteroid revealed by thermochronometry," Nature **422** (6931), 502–506 (2003).

M. Trieloff, E. V. Korochantseva, A. I. Buikin, J. Hopp, M. A. Ivanova, and A. V. Korochantsev, "The Chelyabinsk meteorite: Thermal history and variable shock effects recorded by the ^{40}Ar–^{39}Ar system," Meteorit. Planet. Sci. **53** (3), 343–358 (2018).

A. B. Verchovsky, "Origin of isotopically light nitrogen in meteorites," Geochem. Int. **55** (11), 957–970 (2017).

A. B. Verchovsky, A. V. Fisenko, L. F. Semjonova, I. P. Wright, M. R. Lee, and C. T. Pillinger, "C, N, and noble gas isotopes in grain size separates of presolar diamonds from Efremovka," Science **281** (5380), 1165–1168 (1998).

M. K. Weisberg, C. Smith, G. Benedix, L. Folco, K. Righter, J. Zipfel, A. Yamaguchi, and Aoudjehane H. Chennaoui, "The Meteoritical Bulletin, No. 95," Meteorit. Planet. Sci. **44** (3), 429–462 (2009).

R. Wieler, H. Baur, and P. Signer, "Noble gases from solar energetic particles revealed by closed system stepwise etching of lunar soil minerals," Geochim. Cosmochim. Acta. **50** (9), 1997–2017 (1986).

I. P. Wright and C. T. Pillinger, "Carbon isotopic analysis of small samples by use of stepped-heating extraction and static mass spectrometry," U.S. Geol. Bull., No. 7890, 9–34 (1989).

I. P. Wright, S. R. Boyd, I. A. Franchi, and C. T. Pillinger, "High precision determination of nitrogen stable isotope ratios at the sub-nanomole level," J. Physics E. **21**, 865–875 (1988).

J. Yang, Y. T. Lin, K. H. Joy, and B. Chen, "The petrogenesis of very low-Ti mare basaltic clasts in lunar meteorite Dhofar 1442," *50th Lunar and Planetary Science Conference,* abstract #6258 (2019).

R. A. Zeigler, R. L. Korotev, and B. L. Jolliff, "Petrography and geochemistry of lunar meteorite Dhofar 1442," *42nd Lunar and Planetary Science Conference*, abstract#1012 (2011).

Q. Zhou, R. A. Zeigler, Q. -Z. Yin, R. L. Korotev, B. L. Jolliff, Y. Amelin, K. Marti, F. Y. Wu, X. H. Li, Q. L. Li, Y. T. Lin, Y. Liu, and G. Q. Tang, "U–Pb dating of zircons and phosphates in lunar meteorites, acapulcoites and angrites," *43rd Lunar and Planetary Science Conference,* abstract #1554 (2012).

Q. Zhou, Q. Z. Yin, R. Zeigler, R. Korotev, B. Jolliff, F. Y. Wu, X. H. Li, Q. L. Li, Y. Liu, G. Q. Tang, and C. L. Li, "U–Pb dating of phosphates in lunar meteorite Dhofar 1442," *46th Lunar and Planetary Science Conference,* abstract #1771 (2015).

Translated by M. Bogina